NUWC-NPT Technical Report 12,039
11 April 2011

Elastic Response of a Cylinder Containing Longitudinal Stiffeners

Andrew J. Hull
Autonomous and Defensive Systems Department

Naval Undersea Warfare Center Division
Newport, Rhode Island

PREFACE

This report was funded by the Naval Undersea Warfare Center's In-House Laboratory Independent Research (ILIR) Program, program manager Anthony A. Ruffa (Code 01CTO).

The technical reviewer for this report was Paul V. Cavallaro (Code 70T).

The author wishes to thank Anthony S. Poirier (Code 74) for providing the finite element analysis results.

Reviewed and Approved: 11 April 2011

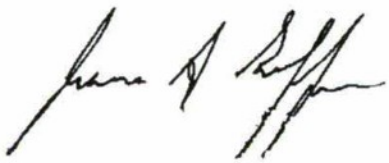

James S. Griffin
Head, Autonomous and Defensive Systems Department

REPORT DOCUMENTATION PAGE

Form Approved
OMB No. 0704-0188

1. REPORT DATE (*DD-MM-YYYY*)	2. REPORT TYPE	3. DATES COVERED (*From – To*)
11-04-2011		

4. TITLE AND SUBTITLE

Elastic Response of a Cylinder Containing Longitudinal Stiffeners

5a. CONTRACT NUMBER

5b. GRANT NUMBER

5c. PROGRAM ELEMENT NUMBER

6. AUTHOR(S)

Andrew J. Hull

5. d PROJECT NUMBER

5e. TASK NUMBER

5f. WORK UNIT NUMBER

7. PERFORMING ORGANIZATION NAME(S) AND ADDRESS(ES)

Naval Undersea Warfare Center Division
1176 Howell Street
Newport, RI 02841-1708

8. PERFORMING ORGANIZATION REPORT NUMBER

TR 12,039

9. SPONSORING/MONITORING AGENCY NAME(S) AND ADDRESS(ES)

10. SPONSORING/MONITOR'S ACRONYM

11. SPONSORING/MONITORING REPORT NUMBER

12. DISTRIBUTION/AVAILABILITY STATEMENT

Approved for public release; distribution is unlimited.

13. SUPPLEMENTARY NOTES

14. ABSTRACT

This report develops a three-dimensional analytical model of a cylinder that contains a longitudinal stiffener. The model begins with the equations of motion for a fully-elastic solid that produces displacement fields with unknown wave propagation coefficients. These are inserted into stress and displacement equations at the cylinder boundaries and at the location of the stiffener. Orthogonalization of these equations produces an infinite number of indexed algebraic equations that can be truncated and incorporated into a global matrix equation. Solving this equation yields the solution to the wave propagation coefficients and allows the systems' displacements and stresses to be calculated. The model is verified by comparison of the results of a plane strain analysis example to a solution generated using finite element theory. An example problem is formulated and the displacement results are illustrated. The inclusion of multiple stiffeners is discussed.

15. SUBJECT TERMS

Fully-elastic cylinder Stiffener Analytical model

16. SECURITY CLASSIFICATION OF:			17. LIMITATION OF ABSTRACT	18. NUMBER OF PAGES	19a. NAME OF RESPONSIBLE PERSON
a. REPORT	b. ABSTRACT	c. THIS PAGE			Andrew J. Hull
(U)	(U)	(U)	SAR	40	19b. TELEPHONE NUMBER (*Include area code*) (401) 832-5189

TABLE OF CONTENTS

LIST OF ILLUSTRATIONS

ELASTIC RESPONSE OF A CYLINDER CONTAINING LONGITUDINAL STIFFENERS

1. INTRODUCTION

Cylindrical shell theories have been developed over a number of years and there exists a large quantity of these theories (reference 1) to model the response of thin shells to free-wave propagation and various external loading conditions. Thin shell theories usually involve a flexural wave propagating in the shell's axial direction and they sometimes include waves propagating in the circumferential direction. Fully-elastic isotropic (thick) shell theory has also been developed (reference 2) and this allows for higher-order wave motion in the radial direction, which results in significant displacement and stress differences in this direction. Transversely-isotropic shell theory has been formulated (reference 3) for shells that have different moduli in the axial direction than the radial and circumferential direction. The reaction of orthotropic cylinder response has been derived (reference 4) for shells that have different moduli in all three of the shell's primary directions. The above references all consider the shell material properties to be homogeneous in each specific direction, although for the latter documents (references 3 and 4) these properties do not necessarily have to be equal.

Shells can be reinforced with external or internal stiffeners to add strength and reduce weight. Circumferential stiffeners have been added to a thin shell energy model (reference 5) to determine the system's stop and pass bands and this was specifically applied to aircraft fuselages. Circumferential stiffeners have been added to a thin shell finite element model (reference 6) and this resulted in identification of stop and pass bands and the amount of coupling between the specific modes. Free vibration of longitudinally-stiffened thin cylindrical shells was investigated using Donnell shell equations (reference 7) and the results were compared to an analytical solution generated using a Ritz solution method. Axial stiffeners have been added to a thin shell energy method (reference 8) to determine the system's pass and stop bands using a variety of different stiffener shapes. A study of Timoshenko-Mindlin type shell with an internal, lengthwise rib has been undertaken (reference 9) to compute the resonances as a function of wave radius and shell angle. An analytical method for longitudinally-stiffened shells to predict modal density and radiation efficiency for use with statistical energy analysis has been developed recently (reference 10). Note that references 5 to 10 are all some type of thin shell theory and the reinforcement is external to the cylinder medium.

This report derives an analytical model of a fully-elastic cylindrical shell that contains a longitudinal stiffener at some location in the shell's interior. The governing equations of the shell are the Navier-Cauchy equations of motion in cylindrical coordinates and the governing equations of the stiffener are the bar (wave) equation in the longitudinal direction and mass multiplied by acceleration in the radial and circumferential directions. The shell is divided into two separate cylinders so that the stiffener lies on the exterior surface of the inner cylinder and the interior surface of the outer cylinder. This allows the displacements to be written without the stiffener forces as functions of the radial, circumferential, and longitudinal directions with

unknown wave propagation coefficients on both of the mediums. Once these are formulated, twelve boundary value equations are written using these displacements or their derivatives. The equations that couple the inner and outer cylinder stresses contain the forces of the stiffener. These equations are solved using an orthogonalization procedure, and this results in the solution of the wave propagation coefficients. These are inserted back into the original displacement equations and this produces known displacements and stresses. The model is validated by comparing a zero wavenumber (plane strain) excitation to a solution obtained using finite element analysis. An example problem is formulated and analyzed. The addition of multiple stiffeners into the model is also discussed.

2. SYSTEM MODEL

The system model is that of a cylinder containing a longitudinal stiffener, as shown in figure 1. This problem is analytically modeled by assuming that the cylinder is governed by fully-elastic equations of motion and the stiffener is modeled using the bar wave equation for its axial (extensional) motion and line mass equations for its non-axial motion. The model uses the following assumptions: (1) the cylinder has infinite spatial extent in the axial direction; (2) the displacements in the cylinder are linear and three-dimensional; (3) the longitudinal stiffener is continuous and it exerts forces in the radial, circumferential, and axial directions on the cylinder, and; (4) the stiffener's cross-sectional area is sufficiently small that it can be modeled as a point force in the radial and circumferential directions.

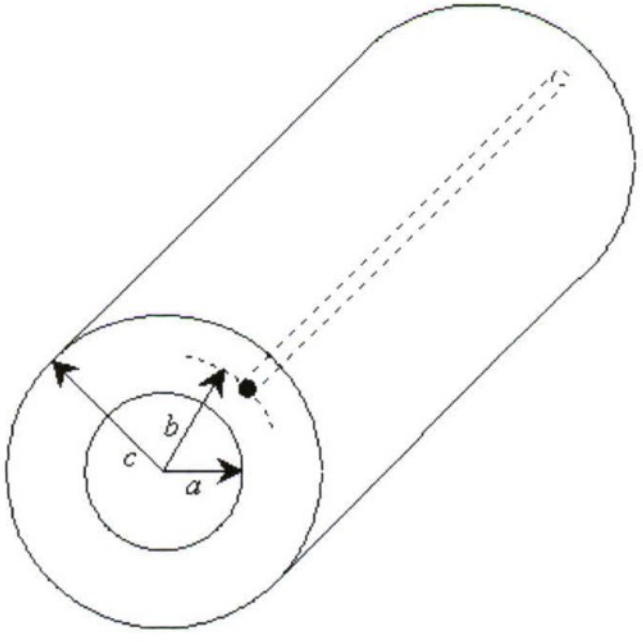

Figure 1. Schematic of a Modeled System

The cylinder's motion is governed by the Navier-Cauchy equations of motion written in vector form as

$$\mu\nabla^2\mathbf{u}(r,\theta,z,t)+(\lambda+\mu)\nabla\nabla\bullet\mathbf{u}(r,\theta,z,t)=\rho\frac{\partial^2\mathbf{u}(r,\theta,z,t)}{\partial t^2}\ , \tag{1}$$

where ρ is density, λ and μ are Lamé constants, r is the radial direction, θ is the circumferential direction, z is the axial direction, t is time, and $\mathbf{u}$ is the cylindrical coordinate displacement vector. Using previously-developed techniques (references 11 and 12), and separating the domain into two regions based on the radial location of the stiffener b, the radial displacement can be written as

$$u_j(r,\theta,z,t)=\sum_{m=-\infty}^{m=+\infty}U_m^{(j)}(r)\exp(\mathrm{i}m\theta)\exp(\mathrm{i}kz)\exp(-\mathrm{i}\omega t)\ , \tag{2}$$

where $a\le r\le b$ is denoted region (j =) 1 and the radial dependency of equation (2) is written as

$$U_m^{(1)}(r)=A_m\left[-\alpha\,\mathrm{J}_{m+1}(\alpha r)+\left(\frac{m}{r}\right)\mathrm{J}_m(\alpha r)\right]+B_m\left[-\alpha\,\mathrm{Y}_{m+1}(\alpha r)+\left(\frac{m}{r}\right)\mathrm{Y}_m(\alpha r)\right]$$
$$+C_m\left(\frac{\mathrm{i}m}{r}\right)\mathrm{J}_m(\beta r)+D_m\left(\frac{\mathrm{i}m}{r}\right)\mathrm{Y}_m(\beta r)+E_m(\mathrm{i}k)\mathrm{J}_{m+1}(\beta r)+F_m(\mathrm{i}k)\mathrm{Y}_{m+1}(\beta r) \tag{3}$$

and where $b\le r\le c$ is denoted region 2 and the radial dependency of equation (2) is written as

$$U_m^{(2)}(r)=G_m\left[-\alpha\,\mathrm{J}_{m+1}(\alpha r)+\left(\frac{m}{r}\right)\mathrm{J}_m(\alpha r)\right]+H_m\left[-\alpha\,\mathrm{Y}_{m+1}(\alpha r)+\left(\frac{m}{r}\right)\mathrm{Y}_m(\alpha r)\right]$$
$$+K_m\left(\frac{\mathrm{i}m}{r}\right)\mathrm{J}_m(\beta r)+L_m\left(\frac{\mathrm{i}m}{r}\right)\mathrm{Y}_m(\beta r)+M_m(\mathrm{i}k)\mathrm{J}_{m+1}(\beta r)+N_m(\mathrm{i}k)\mathrm{Y}_{m+1}(\beta r)\,. \tag{4}$$

The circumferential (tangential) displacement can be written as

$$v_j(r,\theta,z,t)=\sum_{m=-\infty}^{m=+\infty}V_m^{(j)}(r)\exp(\mathrm{i}m\theta)\exp(\mathrm{i}kz)\exp(-\mathrm{i}\omega t)\ , \tag{5}$$

where $a\le r\le b$ the radial dependency of equation (5) is written as

$$V_m^{(1)}(r) = A_m\left(\frac{\mathrm{i}m}{r}\right)\mathrm{J}_m(\alpha r) + B_m\left(\frac{\mathrm{i}m}{r}\right)\mathrm{Y}_m(\alpha r) + C_m\left[\beta\,\mathrm{J}_{m+1}(\beta r) - \left(\frac{m}{r}\right)\mathrm{J}_m(\beta r)\right]$$
$$+ D_m\left[\beta\,\mathrm{Y}_{m+1}(\beta r) - \left(\frac{m}{r}\right)\mathrm{Y}_m(\beta r)\right] + E_m(\mathrm{i}k)\,\mathrm{J}_{m+1}(\beta r) + F_m(\mathrm{i}k)\mathrm{Y}_{m+1}(\beta r) \qquad (6)$$

and where $b \le r \le c$ the radial dependency of equation (5) is written as

$$V_m^{(2)}(r) = G_m\left(\frac{\mathrm{i}m}{r}\right)\mathrm{J}_m(\alpha r) + H_m\left(\frac{\mathrm{i}m}{r}\right)\mathrm{Y}_m(\alpha r) + K_m\left[\beta\,\mathrm{J}_{m+1}(\beta r) - \left(\frac{m}{r}\right)\mathrm{J}_m(\beta r)\right]$$
$$+ L_m\left[\beta\,\mathrm{Y}_{m+1}(\beta r) - \left(\frac{m}{r}\right)\mathrm{Y}_m(\beta r)\right] + M_m(\mathrm{i}k)\,\mathrm{J}_{m+1}(\beta r) + N_m(\mathrm{i}k)\mathrm{Y}_{m+1}(\beta r)\,. \qquad (7)$$

The axial (longitudinal) displacement can be written as

$$w_j(r,\theta,z,t) = \sum_{m=-\infty}^{m=+\infty} W_m^{(j)} \exp(\mathrm{i}m\theta)\exp(\mathrm{i}kz)\exp(-\mathrm{i}\omega t)\ , \qquad (8)$$

where $a \le r \le b$ the radial dependency of equation (8) is written as

$$W_m^{(j)}(r) = A_m(\mathrm{i}k)\,\mathrm{J}_m(\alpha r) + B_m(\mathrm{i}k)\,\mathrm{Y}_m(\alpha r) + E_m\left[\left(\frac{(1-\mathrm{i})m}{r}\right)\mathrm{J}_{m+1}(\beta r) - \beta\,\mathrm{J}_m(\beta r)\right]$$
$$+ F_m\left[\left(\frac{(1-\mathrm{i})m}{r}\right)\mathrm{Y}_{m+1}(\beta r) - \beta\,\mathrm{Y}_m(\beta r)\right] \qquad (9)$$

and where $b \le r \le c$ the radial dependency of equation (8) is written as

$$W_m^{(j)}(r) = G_m(\mathrm{i}k)\,\mathrm{J}_m(\alpha r) + H_m(\mathrm{i}k)\,\mathrm{Y}_m(\alpha r) + M_m\left[\left(\frac{(1-\mathrm{i})m}{r}\right)\mathrm{J}_{m+1}(\beta r) - \beta\,\mathrm{J}_m(\beta r)\right]$$
$$+ N_m\left[\left(\frac{(1-\mathrm{i})m}{r}\right)\mathrm{Y}_{m+1}(\beta r) - \beta\,\mathrm{Y}_m(\beta r)\right]. \qquad (10)$$

In the above equations, a is the inner radius of the cylinder, b is the radial location of the stiffener, c is the outer radius of the cylinder, α is the modified wavenumber associated with the dilatational wave, β is the modified wavenumber associated with the shear wave, k is the axial wavenumber, ω is the frequency, J_m is an mth order standard Bessel function of the first kind, Y_m is an mth order standard Bessel function of the second kind, and A_m, B_m, C_m, D_m, E_m, F_m, G_m, H_m, K_m, L_m, M_m and N_m are unknown wave propagation coefficients whose solutions are determined below. The modified dilatational wavenumber is calculated using

$$\alpha = \sqrt{\frac{\omega^2}{c_d^2} - k^2} \tag{11}$$

where

$$c_d = \sqrt{\frac{\lambda + 2\mu}{\rho}} \ , \tag{12}$$

and the modified shear wavenumber is calculated using

$$\beta = \sqrt{\frac{\omega^2}{c_s^2} - k^2} \tag{13}$$

where

$$c_s = \sqrt{\frac{\mu}{\rho}} \ . \tag{14}$$

Note that imaginary arguments in the Bessel functions are permissible. For the remainder of this report, the exponentials, with respect to time, are suppressed in all of the equations.

The solution to the wave propagation coefficients are found using 12 boundary value equations that are written using the stress-strain and displacement relations at the locations of the shell's inner radius ($r = a$), location of the stiffener ($r = b$), and the outer radius of the shell ($r = c$). At the inner radius of the shell ($r = a$), the cylinder is modeled as a free surface and the normal stress in the radial direction is

$$\tau_{rr}(a,\theta,z) = (\lambda + 2\mu)\frac{\partial u_1(a,\theta,z)}{\partial r} + \frac{\lambda}{a}u_1(a,\theta,z) + \frac{\lambda}{a}\frac{\partial v_1(a,\theta,z)}{\partial \theta} + \lambda\frac{\partial w_1(a,\theta,z)}{\partial z} = 0 \ , \tag{15}$$

and the shear stresses associated with the radial direction are

$$\tau_{r\theta}(a,\theta,z) = \mu\frac{\partial v_1(a,\theta,z)}{\partial r} - \frac{\mu}{a}v_1(a,\theta,z) + \frac{\mu}{a}\frac{\partial u_1(a,\theta,z)}{\partial \theta} = 0 \tag{16}$$

and

$$\tau_{rz}(a,\theta,z) = \mu\frac{\partial u_1(a,\theta,z)}{\partial z} + \mu\frac{\partial w_1(a,\theta,z)}{\partial r} = 0 \ . \tag{17}$$

At the radial location of the stiffener ($r = b$), three stress balances are written that equate the forces in the embedded stiffener to the stresses in each region of the cylinder. The normal stress in the radial direction is

$$(\lambda+2\mu)\frac{\partial u_1(b,\theta,z)}{\partial r}+\frac{\lambda}{b}u_1(b,\theta,z)+\frac{\lambda}{b}\frac{\partial v_1(b,\theta,z)}{\partial \theta}+\lambda\frac{\partial w_1(b,\theta,z)}{\partial z}$$
$$=(\lambda+2\mu)\frac{\partial u_2(b,\theta,z)}{\partial r}+\frac{\lambda}{b}u_2(b,\theta,z)+\frac{\lambda}{b}\frac{\partial v_2(b,\theta,z)}{\partial \theta}$$
$$+\lambda\frac{\partial w_2(b,\theta,z)}{\partial z}-f_r(b,\theta,z)\delta(\theta-\theta_0)\,, \tag{18}$$

and the shear stresses associated with the radial direction are

$$\mu\frac{\partial v_1(b,\theta,z)}{\partial r}-\frac{\mu}{b}v_1(b,\theta,z)+\frac{\mu}{b}\frac{\partial u_1(b,\theta,z)}{\partial \theta}$$
$$=\mu\frac{\partial v_2(b,\theta,z)}{\partial r}-\frac{\mu}{b}v_2(b,\theta,z)+\frac{\mu}{b}\frac{\partial u_2(b,\theta,z)}{\partial \theta}-f_\theta(b,\theta,z)\delta(\theta-\theta_0) \tag{19}$$

and

$$\mu\frac{\partial u_1(b,\theta,z)}{\partial z}+\mu\frac{\partial w_1(b,\theta,z)}{\partial r}$$
$$=\mu\frac{\partial u_2(b,\theta,z)}{\partial z}+\mu\frac{\partial w_2(b,\theta,z)}{\partial r}-f_z(b,\theta,z)\delta(\theta-\theta_0)\,. \tag{20}$$

where $f_r(b,\theta,z)$, $f_\theta(b,\theta,z)$, and $f_z(b,\theta,z)$ are the radial, circumferential, and longitudinal stresses, respectively, that the embedded stiffener exerts on the shell, δ is the Dirac delta function and θ_0 is the angular offset of the stiffener with respect to $\theta = 0$. At the stiffener's radial location, three equations are written that equate the displacement continuity from the first region to the second region. These equations are

$$u_1(b,\theta,z)=u_2(b,\theta,z)\,, \tag{21}$$

$$v_1(b,\theta,z)=v_2(b,\theta,z)\,, \tag{22}$$

and

$$w_1(b,\theta,z)=w_2(b,\theta,z)\,. \tag{23}$$

At the outer radius of the shell ($r = c$), the cylinder is modeled as a free surface with an applied radial stress. The normal stress in the radial direction is

$$\tau_{rr}(c,\theta,z) = (\lambda + 2\mu)\frac{\partial u_2(c,\theta,z)}{\partial r} + \frac{\lambda}{c}u_2(c,\theta,z) + \frac{\lambda}{c}\frac{\partial v_2(c,\theta,z)}{\partial \theta} + \lambda\frac{\partial w_2(c,\theta,z)}{\partial z} = p(\theta,z) \ , \tag{24}$$

and the shear stresses associated with the radial direction are

$$\tau_{r\theta}(c,\theta,z) = \mu\frac{\partial v_2(c,\theta,z)}{\partial r} - \frac{\mu}{c}v_2(c,\theta,z) + \frac{\mu}{c}\frac{\partial u_2(c,\theta,z)}{\partial \theta} = 0 \tag{25}$$

and

$$\tau_{rz}(c,\theta,z) = \mu\frac{\partial u_2(c,\theta,z)}{\partial z} + \mu\frac{\partial w_2(c,\theta,z)}{\partial r} = 0 \ . \tag{26}$$

where $p(\theta,z)$ is the applied radial stress at the location $r = c$.

For the embedded stiffener, the internal forces in the radial and circumferential directions are modeled as line masses multiplied by the acceleration in these directions. This is written as

$$f_r(b,\theta,z) = \frac{-\omega^2 M_s}{2\pi b}\sum_{m=-\infty}^{m=+\infty} U_m^{(1)}(b)\exp(\mathrm{i}m\theta)\exp(\mathrm{i}kz) \ , \tag{27}$$

$$f_\theta(b,\theta,z) = \frac{-\omega^2 M_s}{2\pi b}\sum_{m=-\infty}^{m=+\infty} V_m^{(1)}(b)\exp(\mathrm{i}m\theta)\exp(\mathrm{i}kz) \ , \tag{28}$$

where M_s is the mass-per-unit length of the stiffener. Note that if the stiffener has significant bending stiffness, the mass terms in equations (27) and (28) can be replaced by a dynamic beam model such as the Bernoulli-Euler beam equation or the Timoshenko beam equation. The internal forces in the axial direction are modeled using the bar wave equation, and this equation is written as

$$f_z(b,\theta,z) = \frac{(-A_s\rho_s\omega^2 + A_sE_sk^2)}{2\pi b}\sum_{m=-\infty}^{m=+\infty} W_m^{(1)}(b)\exp(\mathrm{i}m\theta)\exp(\mathrm{i}kz) \ , \tag{29}$$

where A_s is the cross-sectional area of the stiffener, ρ_s is the density of the stiffener, and E_s is Young's modulus of the stiffener. For the numerical examples presented here, the external force on the outside of the shell is modeled as a ring pressure with axial wavenumber k, and is given by

$$p(\theta,z) = P_0\exp(\mathrm{i}kz) \ . \tag{30}$$

Using the above four equations, and the functional form of the displacement fields, equations (15) to (26) become

$$\sum_{m=-\infty}^{m=+\infty}\left[(\lambda+2\mu)\frac{\mathrm{d}U_m^{(1)}(a)}{\mathrm{d}r}+\frac{\lambda}{a}U_m^{(1)}(a)+\frac{\mathrm{i}m\lambda}{a}V_m^{(1)}(a)+\mathrm{i}k\lambda W_m^{(1)}(a)\right]\exp(\mathrm{i}m\theta)=0\ , \tag{31}$$

$$\sum_{m=-\infty}^{m=+\infty}\left[\mu\frac{\mathrm{d}V_m^{(1)}(a)}{\mathrm{d}r}-\frac{\mu}{a}V_m^{(1)}(a)+\frac{\mathrm{i}m\mu}{a}U_m^{(1)}(a)\right]\exp(\mathrm{i}m\theta)=0\ , \tag{32}$$

$$\sum_{m=-\infty}^{m=+\infty}\left[\mathrm{i}k\mu U_m^{(1)}(a)+\mu\frac{\mathrm{d}W_m^{(1)}(a)}{\mathrm{d}r}\right]\exp(\mathrm{i}m\theta)=0\ , \tag{33}$$

$$\begin{aligned}&\sum_{m=-\infty}^{m=+\infty}\left[(\lambda+2\mu)\frac{\mathrm{d}U_m^{(1)}(b)}{\mathrm{d}r}+\frac{\lambda}{b}U_m^{(1)}(b)+\frac{\mathrm{i}m\lambda}{b}V_m^{(1)}(b)+\mathrm{i}k\lambda W_m^{(1)}(b)\right]\exp(\mathrm{i}m\theta)\\&\quad-\sum_{m=-\infty}^{m=+\infty}\left[(\lambda+2\mu)\frac{\mathrm{d}U_m^{(2)}(b)}{\mathrm{d}r}+\frac{\lambda}{b}U_m^{(2)}(b)+\frac{\mathrm{i}m\lambda}{b}V_m^{(2)}(b)+\mathrm{i}k\lambda W_m^{(2)}(b)\right]\exp(\mathrm{i}m\theta)\\&\quad=\frac{\omega^2M_s}{2\pi b}\left[\sum_{m=-\infty}^{m=+\infty}U_m^{(1)}(b)\exp(\mathrm{i}m\theta)\right]\delta(\theta-\theta_0)\ ,\end{aligned} \tag{34}$$

$$\begin{aligned}&\sum_{m=-\infty}^{m=+\infty}\left[\mu\frac{\mathrm{d}V_m^{(1)}(b)}{\mathrm{d}r}-\frac{\mu}{b}V_m^{(1)}(b)+\frac{\mathrm{i}m\mu}{b}U_m^{(1)}(b)\right]\exp(\mathrm{i}m\theta)\\&\quad-\sum_{m=-\infty}^{m=+\infty}\left[\mu\frac{\mathrm{d}V_m^{(2)}(b)}{\mathrm{d}r}-\frac{\mu}{b}V_m^{(2)}(b)+\frac{\mathrm{i}m\mu}{b}U_m^{(2)}(b)\right]\exp(\mathrm{i}m\theta)\\&\quad=\frac{\omega^2M_s}{2\pi b}\left[\sum_{m=-\infty}^{m=+\infty}V_m^{(1)}(b)\exp(\mathrm{i}m\theta)\right]\delta(\theta-\theta_0)\ ,\end{aligned} \tag{35}$$

$$\begin{aligned}&\sum_{m=-\infty}^{m=+\infty}\left[\mathrm{i}k\mu U_m^{(1)}(b)+\mu\frac{\mathrm{d}W_m^{(1)}(b)}{\mathrm{d}r}\right]\exp(\mathrm{i}m\theta)\\&\quad-\sum_{m=-\infty}^{m=+\infty}\left[\mathrm{i}k\mu U_m^{(2)}(b)+\mu\frac{\mathrm{d}W_m^{(2)}(b)}{\mathrm{d}r}\right]\exp(\mathrm{i}m\theta)\\&\quad=\frac{(A_s\rho_s\omega^2-A_sE_sk^2)}{2\pi b}\left[\sum_{m=-\infty}^{m=+\infty}W_m^{(1)}(b)\exp(\mathrm{i}m\theta)\right]\delta(\theta-\theta_0)\ ,\end{aligned} \tag{36}$$

$$\sum_{m=-\infty}^{m=+\infty} U_m^{(1)}(b)\exp(\mathrm{i}m\theta) - \sum_{m=-\infty}^{m=+\infty} U_m^{(2)}(b)\exp(\mathrm{i}m\theta) = 0 \ , \tag{37}$$

$$\sum_{m=-\infty}^{m=+\infty} V_m^{(1)}(b)\exp(\mathrm{i}m\theta) - \sum_{m=-\infty}^{m=+\infty} V_m^{(2)}(b)\exp(\mathrm{i}m\theta) = 0 \ , \tag{38}$$

$$\sum_{m=-\infty}^{m=+\infty} W_m^{(1)}(b)\exp(\mathrm{i}m\theta) - \sum_{m=-\infty}^{m=+\infty} W_m^{(2)}(b)\exp(\mathrm{i}m\theta) = 0 \ , \tag{39}$$

$$\sum_{m=-\infty}^{m=+\infty}\left[(\lambda+2\mu)\frac{\mathrm{d}U_m^{(2)}(c)}{\mathrm{d}r} + \frac{\lambda}{c}U_m^{(2)}(c) + \frac{\mathrm{i}m\lambda}{c}V_m^{(2)}(c) + \mathrm{i}k\lambda W_m^{(2)}(c)\right]\exp(\mathrm{i}m\theta) = P_0 \ , \tag{40}$$

$$\sum_{m=-\infty}^{m=+\infty}\left[\mu\frac{\mathrm{d}V_m^{(2)}(c)}{\mathrm{d}r} - \frac{\mu}{c}V_m^{(2)}(c) + \frac{\mathrm{i}m\mu}{c}U_m^{(2)}(c)\right]\exp(\mathrm{i}m\theta) = 0 \ , \tag{41}$$

and

$$\sum_{m=-\infty}^{m=+\infty}\left[\mathrm{i}k\mu U_m^{(2)}(c) + \mu\frac{\mathrm{d}W_m^{(2)}(c)}{\mathrm{d}r}\right]\exp(\mathrm{i}m\theta) = 0 \ . \tag{42}$$

The presence of the Dirac delta functions in equations (34) to (36) complicates the form of these equations. Converting the delta function to its equivalent Fourier series and rewriting the stiffener force terms will allow the equations to decouple using an orthogonalization procedure. First, the delta function is rewritten using its Fourier expansion on $\theta \in [0,2\pi]$ as

$$\delta(\theta-\theta_0) = \frac{1}{2\pi}\sum_{n=-\infty}^{n=+\infty}\exp[\mathrm{i}n(\theta-\theta_0)] = \frac{1}{2\pi}\sum_{n=-\infty}^{n=+\infty}\exp(-\mathrm{i}n\theta_0)\exp(\mathrm{i}n\theta) \ . \tag{43}$$

Next, the identities

$$\left[\sum_{m=-\infty}^{m=+\infty}\begin{Bmatrix}U_m^{(1)}(b)\\V_m^{(1)}(b)\\W_m^{(1)}(b)\end{Bmatrix}\exp(\mathrm{i}m\theta)\right]\left[\frac{1}{2\pi}\sum_{n=-\infty}^{n=+\infty}\exp(-\mathrm{i}n\theta_0)\exp(\mathrm{i}n\theta)\right]$$

$$=\frac{1}{2\pi}\sum_{n=-\infty}^{n=+\infty}\sum_{m=-\infty}^{m=+\infty}\begin{Bmatrix}U_m^{(1)}(b)\\V_m^{(1)}(b)\\W_m^{(1)}(b)\end{Bmatrix}\exp[\mathrm{i}(n-m)\theta_0]\exp(\mathrm{i}m\theta)\,. \tag{44}$$

are used to convert the double-multiplicative summations into double-embedded summations. The proof of equation (44) is shown in appendix A. These equations are substituted into the right-hand terms of equations (34) to (36), and equations (31) to (42) are multiplied by the exponential $\exp(-\mathrm{i}p\theta)$ and the resulting expressions are integrated over $[0,2\pi]$. Because the exponential functions $\exp(-\mathrm{i}p\theta)$ and $\exp(\mathrm{i}m\theta)$ are orthogonal on this interval when $m \neq p$, equations (31) to (42) decouple into an infinite number of individually p-indexed equations given by

$$(\lambda+2\mu)\frac{\mathrm{d}U_p^{(1)}(a)}{\mathrm{d}r}+\frac{\lambda}{a}U_p^{(1)}(a)+\frac{\mathrm{i}p\lambda}{a}V_p^{(1)}(a)+\mathrm{i}k\lambda W_p^{(1)}(a)=0\,, \tag{45}$$

$$\mu\frac{\mathrm{d}V_p^{(1)}(a)}{\mathrm{d}r}-\frac{\mu}{a}V_p^{(1)}(a)+\frac{\mathrm{i}p\mu}{a}U_p^{(1)}(a)=0\,, \tag{46}$$

$$\mathrm{i}k\mu U_p^{(1)}(a)+\mu\frac{\mathrm{d}W_p^{(1)}(a)}{\mathrm{d}r}=0\,, \tag{47}$$

$$\begin{aligned}&(\lambda+2\mu)\frac{\mathrm{d}U_p^{(1)}(b)}{\mathrm{d}r}+\frac{\lambda}{b}U_p^{(1)}(b)+\frac{\mathrm{i}p\lambda}{b}V_p^{(1)}(b)+\mathrm{i}k\lambda W_p^{(1)}(b)\\&\quad-(\lambda+2\mu)\frac{\mathrm{d}U_p^{(2)}(b)}{\mathrm{d}r}-\frac{\lambda}{b}U_p^{(2)}(b)-\frac{\mathrm{i}p\lambda}{b}V_p^{(2)}(b)-\mathrm{i}k\lambda W_p^{(2)}(b)\\&\quad=\frac{\omega^2 M_s}{2\pi b}\sum_{n=-\infty}^{n=+\infty}\exp[\mathrm{i}(n-p)\theta_0]U_n^{(1)}(b)\,,\end{aligned} \tag{48}$$

$$\mu\frac{\mathrm{d}V_p^{(1)}(b)}{\mathrm{d}r}-\frac{\mu}{b}V_p^{(1)}(b)+\frac{\mathrm{i}p\mu}{b}U_p^{(1)}(b)$$
$$-\mu\frac{\mathrm{d}V_p^{(2)}(b)}{\mathrm{d}r}+\frac{\mu}{b}V_p^{(2)}(b)-\frac{\mathrm{i}p\mu}{b}U_p^{(2)}(b)$$
$$=\frac{\omega^2 M_s}{2\pi b}\sum_{n=-\infty}^{n=+\infty}\exp[\mathrm{i}(n-p)\theta_0]V_n^{(1)}(b)\,, \tag{49}$$

$$\mathrm{i}k\mu U_p^{(1)}(b)+\mu\frac{\mathrm{d}W_p^{(1)}(b)}{\mathrm{d}r}-\mathrm{i}k\mu U_p^{(2)}(b)-\mu\frac{\mathrm{d}W_p^{(2)}(b)}{\mathrm{d}r}$$
$$=\frac{(A_s\rho_s\omega^2-A_sE_sk^2)}{2\pi b}\sum_{n=-\infty}^{n=+\infty}\exp[\mathrm{i}(n-p)\theta_0]W_n^{(1)}(b)\,, \tag{50}$$

$$U_p^{(1)}(b)-U_p^{(2)}(b)=0\,, \tag{51}$$

$$V_p^{(1)}(b)-V_p^{(2)}(b)=0\,, \tag{52}$$

$$W_p^{(1)}(b)-W_p^{(2)}(b)=0\,, \tag{53}$$

$$(\lambda+2\mu)\frac{\mathrm{d}U_p^{(2)}(c)}{\mathrm{d}r}+\frac{\lambda}{c}U_p^{(2)}(c)+\frac{\mathrm{i}p\lambda}{c}V_p^{(2)}(c)+\mathrm{i}k\lambda W_p^{(2)}(c)=\delta_{0p}P_0\,, \tag{54}$$

$$\mu\frac{\mathrm{d}V_p^{(2)}(c)}{\mathrm{d}r}-\frac{\mu}{c}V_p^{(2)}(c)+\frac{\mathrm{i}p\mu}{c}U_p^{(2)}(c)=0\,, \tag{55}$$

and

$$\mathrm{i}k\mu U_p^{(2)}(c)+\mu\frac{\mathrm{d}W_p^{(2)}(c)}{\mathrm{d}r}=0\,. \tag{56}$$

Note that δ_{0p} in equation (54) is the Kronecker delta function.

The left-hand side of equations (45) to (56) are p-indexed and these terms correspond to the dynamics of the shell. The right-hand side the equations (48) to (50) are n-summed and these terms correspond to the stiffener acting on the shell. The functional forms of the displacements

listed in equations (3), (4), (6), (7), (9) and (10) are now inserted into equations (45) to (56), and this results in an the algebraic matrix equation for each individual p-index written as

$$[\mathbf{A}(p)]\{\mathbf{x}_p\} = \delta_{0p}\{\mathbf{p}\} + \sum_{n=-\infty}^{n=+\infty}[\mathbf{F}(n,p)]\{\mathbf{x}_n\} \ , \tag{57}$$

where $[\mathbf{A}(p)]$ is the 12 x 12 matrix that models the dynamic response of the shell, $\{\mathbf{x}_p\}$ is the 12 x 1 vector of unknown wave propagation coefficients, $[\mathbf{F}(n,p)]$ is the 12 x 12 matrix that models the interaction of the forces in the shell and the forces in the stiffener, and $\{\mathbf{p}\}$ is the 12 x 1 vector that models the applied external load. The entries of the matrices and vectors in equation (57) are listed in appendix B. Equation (57) is now written for all values of the p-index, and this results in

$$\hat{\mathbf{A}}\,\hat{\mathbf{x}} = \hat{\mathbf{F}}\,\hat{\mathbf{x}} + \hat{\mathbf{p}} \ , \tag{58}$$

where $\hat{\mathbf{A}}$ is a block diagonal matrix equal to

$$\hat{\mathbf{A}} = \begin{bmatrix} \ddots & \vdots & & \iddots \\ & \mathbf{A}(-1) & \mathbf{0} & \mathbf{0} & \\ \cdots & \mathbf{0} & \mathbf{A}(0) & \mathbf{0} & \cdots \\ & \mathbf{0} & \mathbf{0} & \mathbf{A}(1) & \\ \iddots & \vdots & & \ddots \end{bmatrix} , \tag{59}$$

with $\mathbf{0}$ a 12 x 12 matrix whose entries are all zero, $\hat{\mathbf{F}}$ is a rank-deficient, block-partitioned matrix equal to

$$\hat{\mathbf{F}} = \begin{bmatrix} \ddots & \vdots & & \iddots \\ & \mathbf{F}(-1,-1) & \mathbf{F}(0,-1) & \mathbf{F}(1,-1) & \\ \cdots & \mathbf{F}(-1,0) & \mathbf{F}(0,0) & \mathbf{F}(1,0) & \cdots \\ & \mathbf{F}(-1,1) & \mathbf{F}(0,1) & \mathbf{F}(1,1) & \\ \iddots & \vdots & & \ddots \end{bmatrix} , \tag{60}$$

$\hat{\mathbf{p}}$ is the system excitation vector that models a normal ring load and is equal to

$$\hat{\mathbf{p}} = [\cdots \quad \mathbf{0}^{\mathrm{T}} \quad \{\mathbf{p}\}^{\mathrm{T}} \quad \mathbf{0}^{\mathrm{T}} \quad \cdots]^{\mathrm{T}} \ , \tag{61}$$

with $\mathbf{0}$ as a 12 x 1 vector whose entries are all zero, and $\hat{\mathbf{x}}$ is the vector of unknown wave propagation coefficients and is equal to

$$\hat{\mathbf{x}} = [\cdots \quad \{\mathbf{x}_{-1}\}^{\mathrm{T}} \quad \{\mathbf{x}_0\}^{\mathrm{T}} \quad \{\mathbf{x}_1\}^{\mathrm{T}} \quad \cdots]^{\mathrm{T}} \ , \tag{62}$$

where

$$\mathbf{x}_n = \{A_n \quad B_n \quad C_n \quad D_n \quad E_n \quad F_n \quad G_n \quad H_n \quad K_n \quad L_n \quad M_n \quad N_n\}^{\mathrm{T}} . \tag{63}$$

Note that from equation (58), the addition of the stiffener force terms couples all of the displacement modes together and they do not respond independently, even though the equations themselves are decoupled. The solution to the wave propagation coefficients in equation (62) is now found by truncating the matrices and vectors in equation (58) to a finite number of terms and solving

$$\hat{\mathbf{x}} = [\hat{\mathbf{A}} - \hat{\mathbf{F}}]^{-1} \hat{\mathbf{p}} . \tag{64}$$

Once the wave propagation coefficients are known, the displacement in all three directions and the stress distribution in the cylinder can be calculated.

3. MODEL VALIDATION

The model that was developed in section 2 can be validated for zero wavenumber response (plane strain) by comparing the analytical results to model results calculated using a finite element program. This comparison used a shell where the inner radius is 0.0825 m, the outer radius is 0.0953 m, Young's modulus is 1.55×10^7 N m^{-2}, Poisson' ratio is 0.45, density is 1250 kg m^{-3}, mass-per-unit length of the stiffener is 0.75 kg m^{-1}, the angular offset of the stiffener is $\pi/6$ radians, radial location of the stiffener is 0.0889 m, and the frequency of excitation is 100 Hz. For the zero wavenumber case, the displacements in the axial direction are all zero and the stiffener's axial properties do not enter into the calculations. The finite element model was run using Abaqus version 6.10 finite element program. The model had 6000 plane strain elements, one mass element, 6600 nodes, and was analyzed using the two-dimensional standard steady state dynamics solver.

Figure 2 shows a plot of the transfer function of displacement divided by pressure versus angle at the radial location of 0.0889 m. The solid line is the radial displacement of the analytical model (equation (2)), the dashed line is the circumferential displacement of the analytical model (equation (5)), the solid markers are the radial displacement of the finite element model, and the circular markers are the circumferential displacement of the finite element model. The analytical model was calculated using 27 terms ($-13 \le m \le 13$), which produced a 324 x 324 system matrix. For this validation problem, there is broad based agreement between the analytical model and the finite element model displacements at all locations on the cylinder.

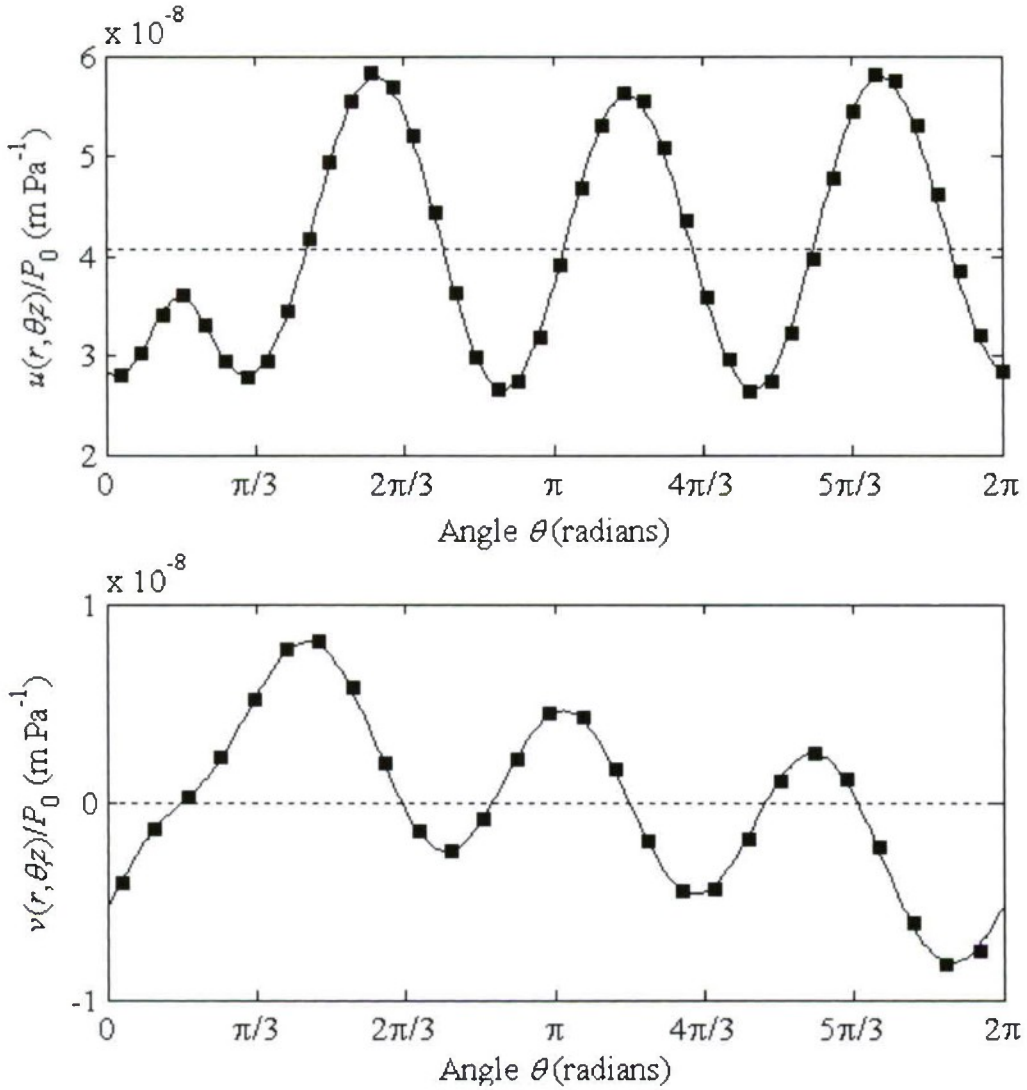

Figure 2. Transfer Function of Radial Displacement Divided by Pressure vs Angle (top) and Circumferential Displacement Divided by Pressure vs Angle (bottom)

Note: In figure 2, the solid line is the analytical model, the square markers are the finite element results, and the dashed line is the response of the cylinder without the stiffener.

4. THREE-DIMENSIONAL ELASTIC EXAMPLE

A three-dimensional example problem is now formulated and discussed. The same parameters used for the shell in the model validation (section 3) are used to construct this numerical example. The embedded stiffener used in this model is Kevlar grade 29 that has a density of 1440 kg m^{-3}, a Young's modulus of 83 x 10^9 N m^{-2}, and a mass-per-unit length of 0.00285 kg m^{-1}. The stiffener has a diameter of 0.00159 m and is in the same physical location as the stiffener in the model in section 3. Figure 3 shows a plot of the magnitude of the transfer functions of displacement divided by pressure versus wavenumber at the location $r = 0.0889$ m, $\theta = \pi/6$ radians, and $z = 0$ m. The plot's scale is in decibels and the units are m Pa^{-1}. The top plot is the radial displacement, the middle plot is the circumferential displacement, and the bottom plot is the longitudinal displacement. The solid lines are the model results with the stiffener and the dashed lines are the model results without the stiffener. The circumferential displacement for the system without the stiffener is zero and thus is not depicted on the middle plot. The analytical model with the stiffeners was calculated using 27 terms and the analytical model without the stiffeners was calculated using a single ($n = 0$) term, as the ring load produces an angularly-symmetric response for the problem without the stiffener and higher order terms do not enter into the analysis. Note in the figures that the resonance for the ring mode has decreased in wavenumber due to the effects of the stiffener. Additionally, the next two modes of the stiffened structure are visible as the response is no longer angularly symmetric.

Figure 4 is a plot of the radial displacement divided by pressure of the stiffened system versus wavenumber and frequency. Figure 5 is a plot of the circumferential displacement divided by pressure versus wavenumber and frequency. Figure 6 is a plot of longitudinal pressure divided by pressure versus wavenumber and frequency. In figures 4 to 6, the location on the cylinder is $r = 0.0889$ m, $\theta = \pi/6$ radians, and $z = 0$ m; the scale of the plot is in decibels; and the units are m Pa^{-1}. For this system, the response is predominantly a combination of the $n = 0$ and $n = 1$ cylinder modes. This was deduced by comparing the $n = 0$ and $n = 1$ modes of the unstiffened system to these figures. The wave speeds of the individual waves, however, have increased with the addition of the stiffener. Note that there is some slight numerical instabilities at extremely low frequencies and high wavenumbers. This is a location (in wavenumber and frequency) that is not typically analyzed because there is no free-wave response in this area.

Three other model attributes are briefly discussed. First, in the event that the cylinder contains Q stiffeners at the radial location $r = b$ and angular location θ_q, the right-hand side of equations (48) to (50) are rewritten as

$$\sum_{q=1}^{q=Q}\left[\frac{\omega^2 M_q}{2\pi b}\sum_{n=-\infty}^{n=+\infty}\exp[\mathrm{i}(n-p)\theta_q]U_n^{(1)}(b)\right], \tag{65}$$

$$\sum_{q=1}^{q=Q}\left[\frac{\omega^2 M_q}{2\pi b}\sum_{n=-\infty}^{n=+\infty}\exp[\mathrm{i}(n-p)\theta_q]V_n^{(1)}(b)\right], \tag{66}$$

and

$$\sum_{q=1}^{q=Q}\left[\frac{(A_q\rho_q\omega^2 - A_qE_qk^2)}{2\pi b}\sum_{n=-\infty}^{n=+\infty}\exp[\mathrm{i}(n-p)\theta_q]W_n^{(1)}(b)\right], \tag{67}$$

where the subscript q corresponds to the qth stiffener. These equations allow additional stiffeners at $r = b$ to be incorporated into the model. Second, if the stiffeners are at a radial location $r \neq b$, then the solution of the cylinder in the radial direction has to be further subdivided at the radial location of each stiffener and six new equations have to be added to the stress and continuity equations for each stiffener when $r \neq a$ or $r \neq c$. These are a radial, circumferential, and longitudinal stress equation and a radial, circumferential, and longitudinal displacement equation. If the stiffener is at the cylinder boundary, i.e. $r = a$ or $r = c$, then only the stress equations are needed to incorporate the effects into the model. Third, if the external load is some function other than a constant ring load, then this function has to be replaced by its Fourier series, then expanded and orthogonalized in a similar manner as to the displacement fields. This process is well known.

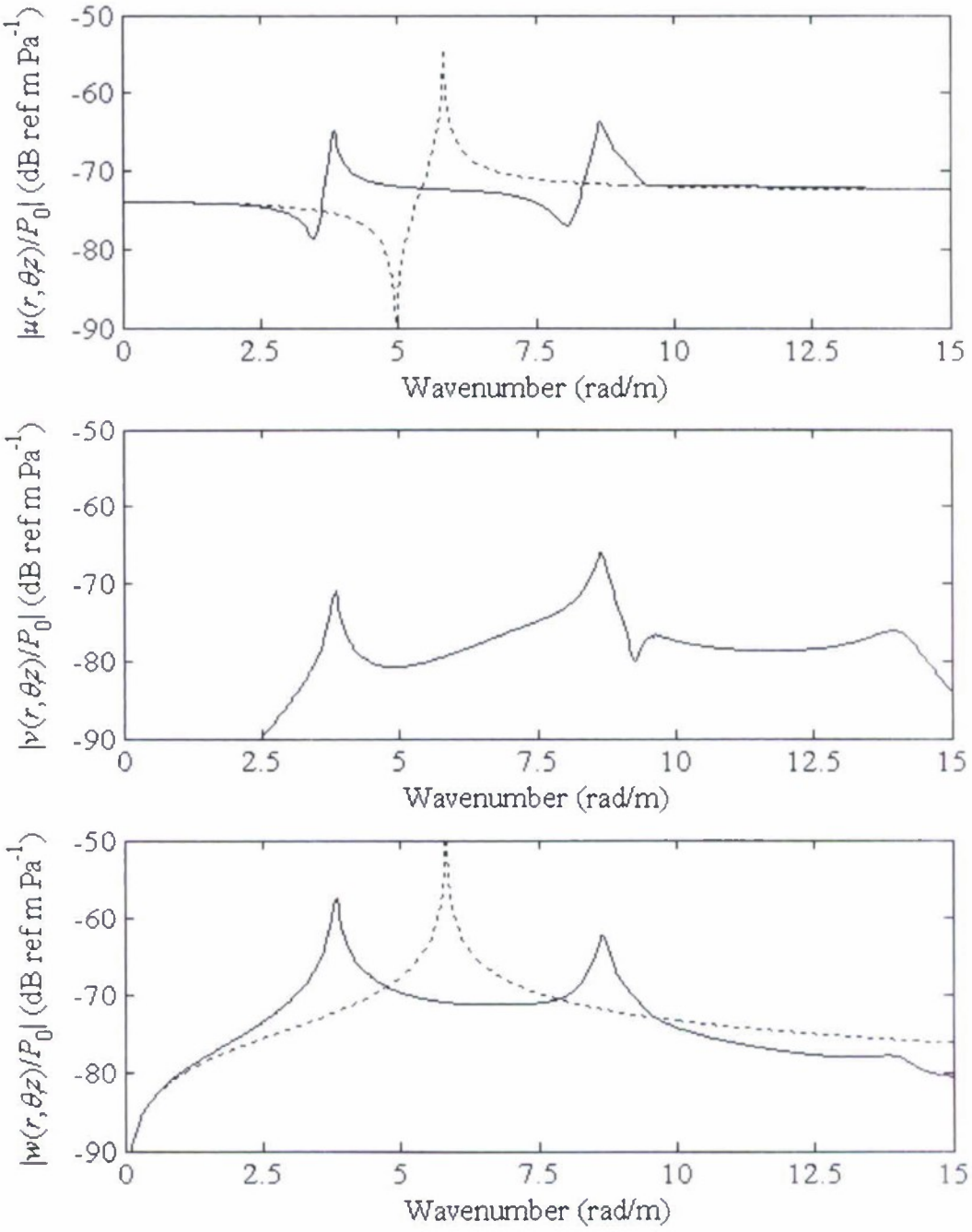

Figure 3. Transfer Function of Displacement Divided by Pressure vs Wavenumber

Note: In figure 3, the top plot is the radial displacement, the middle plot is the circumferential displacement, and the bottom plot is the longitudinal displacement. The solid lines are the model results with the stiffener and the dashed lines are the model results without the stiffener.

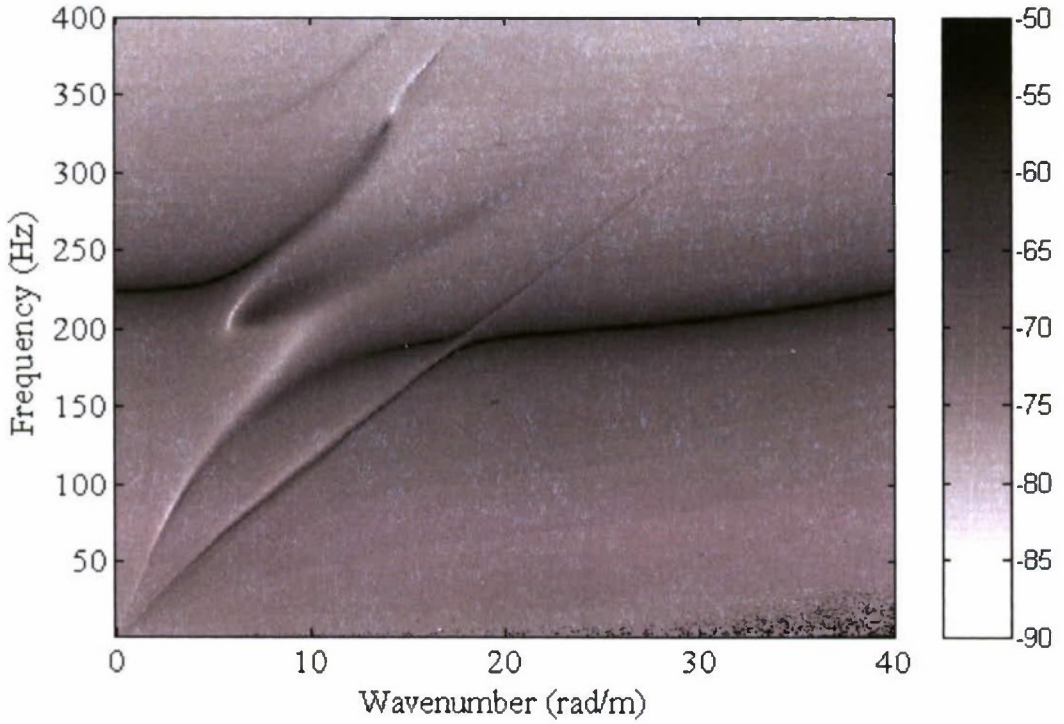

Figure 4. Radial Displacement Divided by Pressure vs Wavenumber and Frequency

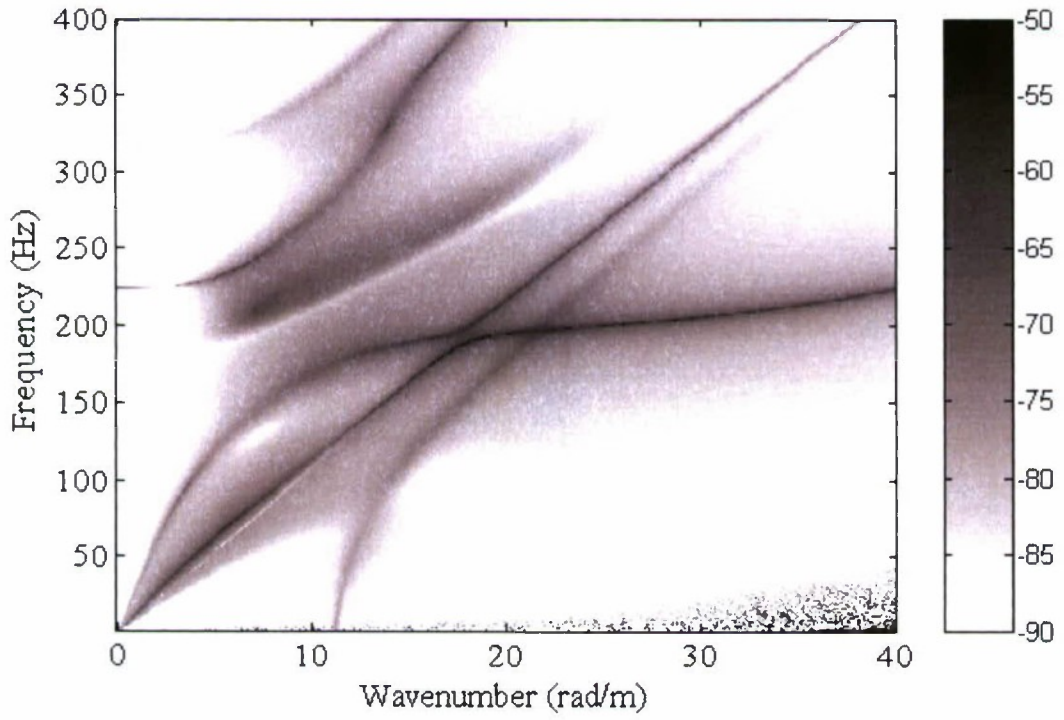

Figure 5. Circumferential Displacement Divided by Pressure vs Wavenumber and Frequency

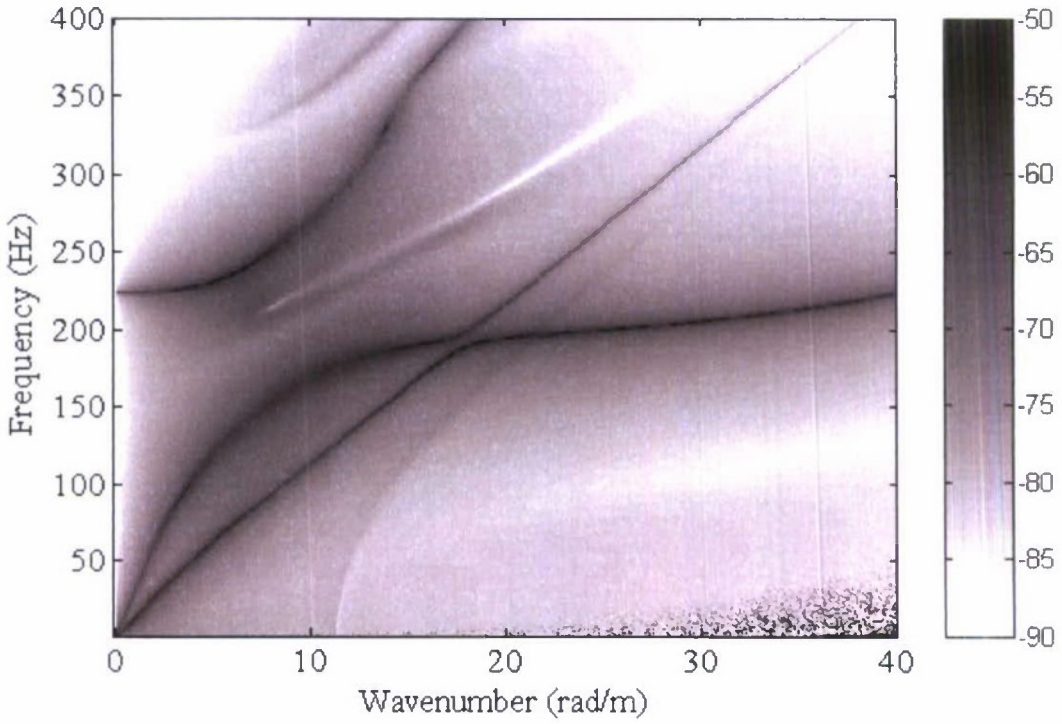

Figure 6. Longitudinal Displacement Divided by Pressure vs Wavenumber and Frequency

5. SUMMARY

An elastic analytieal model of a system that eonsists of a eylinder eontaining an embedded longitudinal stiffener has been derived. This model was developed so that the thick shells that contain one or more stiffeners can be aceurately modeled and analyzed. This new model was verified for the ease of plane strain behavior by comparison of the results to finite element analysis results. An example problem was developed and the behavior of the system at various frequencies and wavenumbers was illustrated. The inelusion of multiple stiffeners was diseussed.

REFERENCES

1. A. Leissa, *Vibration of Shells*, Acoustical Society of America, Melville, New York, 1993.

2. D.C. Gazos, "Three-Dimensional Investigation of the Propagation of Waves In Hollow Circular Cylinders. I. Analytical Formulation," *Journal of the Acoustical Society of America*, vol. 31, no. 5, 1959, pp. 568-573.

3. I. Mirsky, "Wave Propagation in Transversely Isotropic Circular Cylinders Part I: Theory," *Journal of the Acoustical Society of America*, vol. 37, no. 6, 1965, pp. 1016-1021.

4. I. Mirsky, "Axisymmetric Vibrations of Orthotropic Cylinders," *Journal of the Acoustical Society of America*, vol. 36, no. 11, 1964, pp. 2106-2112.

5. D.J. Mead and N.S. Bardell, "Free Vibration of a Thin Cylindrical Shell with Periodic Circumferential Stiffeners," *Journal of Sound and Vibration*, vol. 115, no. 3, 1987, pp. 499-520.

6. M.S. Bennett and M.L. Accorsi, "Free Wave Propagation in Periodically Ring Stiffened Cylindrical Shells," *Journal of Sound and Vibration*, vol. 171, no. 1, 1994, pp. 49-66.

7. J.T.S. Wang and S.A. Rinehart, "Free Vibrations of Longitudinally Stiffened Cylindrical Shells," *Journal of Applied Mechanics*, vol. 41, no. 4, 1974, pp. 1087-1093.

8. D.J. Mead and N.S. Bardell, "Free Vibration of a Thin Cylindrical Shell with Discrete Axial Stiffeners," *Journal of Sound and Vibration*, vol. 111, no. 2, 1986, pp. 229-250.

9. A. Klauson, J. Metsaveer, D. Décultot, G. Maze and J. Ripoche, "Identification of the Resonances of a Cylindrical Shell Stiffened by an Internal Lengthwise Rib," *Journal of the Acoustical Society of America*, vol. 100, no. 5, 1996, pp. 3135-3143.

10. P. Ramachandran and S. Narayanan, "Evaluation of Modal Density, Radiation Efficiency and Acoustic Response of Longitudinally Stiffened Cylindrical Shell," *Journal of Sound and Vibration*, vol. 304, no. 1-2, 2007, pp. 154-174.

11. K.F. Graf, *Wave Motion in Elastic Solids*, Dover Publications, New York, 1975.

12. J.D. Achenbach, *Wave Propagation in Elastic Solids*, North-Holland, The Netherlands, 1975.

APPENDIX A
DOUBLE SUMMATION IDENTITIES

The proof of the double summation identity given in equation (44) is presented in this appendix. The identity is critical in transforming the problem into a form where orthogonal functions can decouple the modes. The first term in equation (44) without the 2π coefficient is

$$\left[\sum_{m=-\infty}^{m=+\infty} X_m \exp(\mathrm{i}m\theta)\right]\left[\sum_{n=-\infty}^{n=+\infty} \exp(-\mathrm{i}n\theta_0)\exp(\mathrm{i}n\theta)\right], \tag{A-1}$$

where X_m is either $U_m^{(1)}(b)$, $V_m^{(1)}(b)$ or $W_m^{(1)}(b)$. This can be written as

$$\sum_{n=-\infty}^{n=+\infty}\left[\sum_{m=-\infty}^{m=+\infty} X_m \exp(\mathrm{i}m\theta)\right]\exp(-\mathrm{i}n\theta_0)\exp(\mathrm{i}n\theta)\ . \tag{A-2}$$

Expanding the m indexed series results in

$$\sum_{n=-\infty}^{n=+\infty}[\cdots + X_{-1}\exp[\mathrm{i}(-1)\theta] + X_0\exp[\mathrm{i}(0)\theta] + X_1\exp[\mathrm{i}(1)\theta] + \cdots]\exp(-\mathrm{i}n\theta_0)\exp(\mathrm{i}n\theta)\ . \tag{A-3}$$

Next, expanding the n indexed series yields

$$\begin{aligned}
&\cdots + [\cdots + X_{-1}\exp[\mathrm{i}(-1)\theta] + X_0\exp[\mathrm{i}(0)\theta] + X_1\exp[\mathrm{i}(1)\theta] + \cdots]\exp[-\mathrm{i}(-1)\theta_0]\exp[\mathrm{i}(-1)\theta] \\
&\quad + [\cdots + X_{-1}\exp[\mathrm{i}(-1)\theta] + X_0\exp[\mathrm{i}(0)\theta] + X_1\exp[\mathrm{i}(1)\theta] + \cdots]\exp[-\mathrm{i}(0)\theta_0]\exp[\mathrm{i}(0)\theta] \\
&\quad + [\cdots + X_{-1}\exp[\mathrm{i}(-1)\theta] + X_0\exp[\mathrm{i}(0)\theta] + X_1\exp[\mathrm{i}(1)\theta] + \cdots]\exp[-\mathrm{i}(1)\theta_0]\exp[\mathrm{i}(1)\theta] + \cdots\ ,
\end{aligned} \tag{A-4}$$

and multiplying through gives

$$\begin{aligned}
&\cdots + [\cdots + X_{-1}\exp[-\mathrm{i}(-1)\theta_0]\exp[\mathrm{i}(-2)\theta] + X_0\exp[-\mathrm{i}(-1)\theta_0]\exp[\mathrm{i}(-1)\theta] \\
&\qquad + X_1\exp[-\mathrm{i}(-1)\theta_0]\exp[\mathrm{i}(0)\theta] + \cdots] \\
&\quad + [\cdots + X_{-1}\exp[-\mathrm{i}(0)\theta_0]\exp[\mathrm{i}(-1)\theta] + X_0\exp[-\mathrm{i}(0)\theta_0]\exp[\mathrm{i}(0)\theta] \\
&\qquad + X_1\exp[-\mathrm{i}(0)\theta_0]\exp[\mathrm{i}(1)\theta] + \cdots] \\
&\quad + [\cdots + X_{-1}\exp[-\mathrm{i}(1)\theta_0]\exp[\mathrm{i}(0)\theta] + X_0\exp[-\mathrm{i}(1)\theta_0]\exp[\mathrm{i}(1)\theta] \\
&\qquad + X_1\exp[-\mathrm{i}(1)\theta_0]\exp[\mathrm{i}(2)\theta] + \cdots] + \cdots\ .
\end{aligned} \tag{A-5}$$

Regrouping equation (A-5) on specific values of X_m yields the equation

$$\cdots + \sum_{m=-\infty}^{m=+\infty} X_{-1} \exp[-\mathrm{i}(m-(-1))\theta_0]\exp[\mathrm{i}m\theta] + \sum_{m=-\infty}^{m=+\infty} X_0 \exp[-\mathrm{i}(m-0)\theta_0]\exp[\mathrm{i}m\theta]$$
$$+ \sum_{m=-\infty}^{m=+\infty} X_1 \exp[-\mathrm{i}(m-1)\theta_0]\exp[\mathrm{i}m\theta] + \ldots \quad , \qquad \text{(A - 6)}$$

which can be rewritten as

$$\sum_{n=-\infty}^{n=+\infty} \sum_{m=-\infty}^{m=+\infty} X_n \exp[\mathrm{i}(n-m)\theta_0]\exp(\mathrm{i}m\theta) \ . \qquad \text{(A-7)}$$

APPENDIX B
MATRIX AND VECTOR ENTRIES

The entries of the matrices and vectors in equation (57) are listed below. The nonzero entries of $[\mathbf{A}(p)]$ are

$$a_{1,1} = \frac{2\mu\alpha}{a} \mathrm{J}_{p+1}(\alpha a) + \left[\frac{2\mu p(p-1)}{a^2} - \alpha^2(\lambda + 2\mu) - \lambda k^2 \right] \mathrm{J}_p(\alpha a) \ , \tag{B-1}$$

$$a_{1,2} = \frac{2\mu\alpha}{a} \mathrm{Y}_{p+1}(\alpha a) + \left[\frac{2\mu p(p-1)}{a^2} - \alpha^2(\lambda + 2\mu) - \lambda k^2 \right] \mathrm{Y}_p(\alpha a) \ , \tag{B-2}$$

$$a_{1,3} = \frac{-2\mathrm{i}\mu\beta p}{a} \mathrm{J}_{p+1}(\beta a) + \frac{2\mathrm{i}\mu p(p-1)}{a^2} \mathrm{J}_p(\beta a) \ , \tag{B-3}$$

$$a_{1,4} = \frac{-2\mathrm{i}\mu\beta p}{a} \mathrm{Y}_{p+1}(\beta a) + \frac{2\mathrm{i}\mu p(p-1)}{a^2} \mathrm{Y}_p(\beta a) \ , \tag{B-4}$$

$$a_{1,5} = \frac{-2\mathrm{i}\mu k(p+1)}{a} \mathrm{J}_{p+1}(\beta a) + 2\mathrm{i}\mu\beta k \, \mathrm{J}_p(\alpha a) \ , \tag{B-5}$$

$$a_{1,6} = \frac{-2\mathrm{i}\mu k(p+1)}{a} \mathrm{Y}_{p+1}(\beta a) + 2\mathrm{i}\mu\beta k \, \mathrm{Y}_p(\alpha a) \ , \tag{B-6}$$

$$a_{2,1} = \frac{-2\mathrm{i}\mu\alpha p}{a} \mathrm{J}_{p+1}(\alpha a) + \frac{2\mathrm{i}\mu p(p-1)}{a^2} \mathrm{J}_p(\alpha a) \ , \tag{B-7}$$

$$a_{2,2} = \frac{-2\mathrm{i}\mu\alpha p}{a} \mathrm{Y}_{p+1}(\alpha a) + \frac{2\mathrm{i}\mu p(p-1)}{a^2} \mathrm{Y}_p(\alpha a) \ , \tag{B-8}$$

$$a_{2,3} = \frac{-2\mu\beta}{a} \mathrm{J}_{p+1}(\beta a) + \left[\frac{-2\mu p(p-1)}{a^2} + \mu\beta^2 \right] \mathrm{J}_p(\beta a) \ , \tag{B-9}$$

$$a_{2,4} = \frac{-2\mu\beta}{a} \mathrm{Y}_{p+1}(\beta a) + \left[\frac{-2\mu p(p-1)}{a^2} + \mu\beta^2 \right] \mathrm{Y}_p(\beta a) \ , \tag{B-10}$$

$$a_{2,5} = \left[\frac{-\mu k p(1+\mathrm{i}) - 2\mathrm{i}\mu k}{a} \right] \mathrm{J}_{p+1}(\beta a) + \mathrm{i}\mu\beta k \, \mathrm{J}_p(\beta a) \ , \tag{B-11}$$

$$a_{2,6} = \left[\frac{-\mu k p(1+\mathrm{i}) - 2\mathrm{i}\mu k}{a} \right] \mathrm{Y}_{p+1}(\beta a) + \mathrm{i}\mu\beta k \, \mathrm{Y}_p(\beta a) \ , \tag{B-12}$$

$$a_{3,1} = -2\mathrm{i}k\mu\alpha \, \mathrm{J}_{p+1}(\alpha a) + \frac{2\mathrm{i}\mu k p}{a} \mathrm{J}_p(\alpha a) \ , \tag{B-13}$$

$$a_{3,2} = -2\mathrm{i}k\mu\alpha \, \mathrm{Y}_{p+1}(\alpha a) + \frac{2\mathrm{i}\mu k p}{a} \mathrm{Y}_p(\alpha a) \ , \tag{B-14}$$

$$a_{3,3} = \frac{-\mu k p}{a} \mathrm{J}_p(\beta a) \ , \tag{B-15}$$

$$a_{3,4} = \frac{-\mu k p}{a} \mathrm{Y}_p(\beta a) \ , \tag{B-16}$$

$$a_{3,5} = \left[\frac{\mu(\mathrm{i}-1)p(p+2)}{a^2} + \mu(\beta^2 - k^2) \right] \mathrm{J}_{p+1}(\beta a) - \frac{\mathrm{i}\mu\beta p}{a} \mathrm{J}_p(\beta a) \ , \tag{B-17}$$

$$a_{3,6} = \left[\frac{\mu(\mathrm{i}-1)p(p+2)}{a^2} + \mu(\beta^2 - k^2) \right] \mathrm{Y}_{p+1}(\beta a) - \frac{\mathrm{i}\mu\beta p}{a} \mathrm{Y}_p(\beta a) \ , \tag{B-18}$$

$$a_{4,1} = \frac{2\mu\alpha}{b} \mathrm{J}_{p+1}(\alpha b) + \left[\frac{2\mu p(p-1)}{b^2} - \alpha^2(\lambda + 2\mu) - \lambda k^2 \right] \mathrm{J}_p(\alpha b) \ , \tag{B-19}$$

$$a_{4,2} = \frac{2\mu\alpha}{b} \mathrm{Y}_{p+1}(\alpha b) + \left[\frac{2\mu p(p-1)}{b^2} - \alpha^2(\lambda + 2\mu) - \lambda k^2 \right] \mathrm{Y}_p(\alpha b) \ , \tag{B-20}$$

$$a_{4,3} = \frac{-2i\mu\beta p}{b} J_{p+1}(\beta b) + \frac{2i\mu p(p-1)}{b^2} J_p(\beta b) \ , \tag{B-21}$$

$$a_{4,4} = \frac{-2i\mu\beta p}{b} Y_{p+1}(\beta b) + \frac{2i\mu p(p-1)}{b^2} Y_p(\beta b) \ , \tag{B-22}$$

$$a_{4,5} = \frac{-2i\mu k(p+1)}{b} J_{p+1}(\beta b) + 2i\mu\beta k J_p(\beta b) \ , \tag{B-23}$$

$$a_{4,6} = \frac{-2i\mu k(p+1)}{b} Y_{p+1}(\beta b) + 2i\mu\beta k Y_p(\beta b) \ , \tag{B-24}$$

$$a_{4,7} = -a_{4,1} \ , \tag{B-25}$$

$$a_{4,8} = -a_{4,2} \ , \tag{B-26}$$

$$a_{4,9} = -a_{4,3} \ , \tag{B-27}$$

$$a_{4,10} = -a_{4,4} \ , \tag{B-28}$$

$$a_{4,11} = -a_{4,5} \ , \tag{B-29}$$

$$a_{4,12} = -a_{4,6} \ , \tag{B-30}$$

$$a_{5,1} = \frac{-2i\mu\alpha p}{b} J_{p+1}(\alpha b) + \frac{2i\mu p(p-1)}{b^2} J_p(\alpha b) \ , \tag{B-31}$$

$$a_{5,2} = \frac{-2i\mu\alpha p}{b} Y_{p+1}(\alpha b) + \frac{2i\mu p(p-1)}{b^2} Y_p(\alpha b) \ , \tag{B-32}$$

$$a_{5,3} = \frac{-2\mu\beta}{b} \mathrm{J}_{p+1}(\beta b) + \left[\frac{-2\mu p(p-1)}{b^2} + \mu\beta^2 \right] \mathrm{J}_p(\beta b) \ , \tag{B-33}$$

$$a_{5,4} = \frac{-2\mu\beta}{b} \mathrm{Y}_{p+1}(\beta b) + \left[\frac{-2\mu p(p-1)}{b^2} + \mu\beta^2 \right] \mathrm{Y}_p(\beta b) \ , \tag{B-34}$$

$$a_{5,5} = \left[\frac{-\mu k p(1+\mathrm{i}) - 2\mathrm{i}\mu k}{b} \right] \mathrm{J}_{p+1}(\beta b) + \mathrm{i}\mu\beta k \, \mathrm{J}_p(\beta b) \ , \tag{B-35}$$

$$a_{5,6} = \left[\frac{-\mu k p(1+\mathrm{i}) - 2\mathrm{i}\mu k}{b} \right] \mathrm{Y}_{p+1}(\beta b) + \mathrm{i}\mu\beta k \, \mathrm{Y}_p(\beta b) \ , \tag{B-36}$$

$$a_{5,7} = -a_{5,1} \ , \tag{B-37}$$

$$a_{5,8} = -a_{5,2} \ , \tag{B-38}$$

$$a_{5,9} = -a_{5,3} \ , \tag{B-39}$$

$$a_{5,10} = -a_{5,4} \ , \tag{B-40}$$

$$a_{5,11} = -a_{5,5} \ , \tag{B-41}$$

$$a_{5,12} = -a_{5,6} \ , \tag{B-42}$$

$$a_{6,1} = -2\mathrm{i}k\mu\alpha \, \mathrm{J}_{p+1}(\alpha b) + \frac{2\mathrm{i}\mu k p}{b} \mathrm{J}_p(\alpha b) \ , \tag{B-43}$$

$$a_{6,2} = -2\mathrm{i}k\mu\alpha \, \mathrm{Y}_{p+1}(\alpha b) + \frac{2\mathrm{i}\mu k p}{b} \mathrm{Y}_p(\alpha b) \ , \tag{B-44}$$

$$a_{6,3} = \frac{-\mu k p}{b} \mathrm{J}_p(\beta b) \ , \tag{B-45}$$

$$a_{6,4} = \frac{-\mu k p}{b} \mathrm{Y}_p(\beta b) \ , \tag{B-46}$$

$$a_{6,5} = \left[\frac{\mu(\mathrm{i}-1)p(p+2)}{b^2} + \mu(\beta^2 - k^2) \right] \mathrm{J}_{p+1}(\beta b) - \frac{\mathrm{i}\mu\beta p}{b} \mathrm{J}_p(\beta b) \ , \tag{B-47}$$

$$a_{6,6} = \left[\frac{\mu(\mathrm{i}-1)p(p+2)}{b^2} + \mu(\beta^2 - k^2) \right] \mathrm{Y}_{p+1}(\beta b) - \frac{\mathrm{i}\mu\beta p}{b} \mathrm{Y}_p(\beta b) \ , \tag{B-48}$$

$$a_{6,7} = -a_{6,1} \ , \tag{B-49}$$

$$a_{6,8} = -a_{6,2} \ , \tag{B-50}$$

$$a_{6,9} = -a_{6,3} \ , \tag{B-51}$$

$$a_{6,10} = -a_{6,4} \ , \tag{B-52}$$

$$a_{6,11} = -a_{6,5} \ , \tag{B-53}$$

$$a_{6,12} = -a_{6,6} \ , \tag{B-54}$$

$$a_{7,1} = -\alpha \mathrm{J}_{p+1}(\alpha b) + \frac{p}{b} \mathrm{J}_p(\alpha b) \ , \tag{B-55}$$

$$a_{7,2} = -\alpha \mathrm{Y}_{p+1}(\alpha b) + \frac{p}{b} \mathrm{Y}_p(\alpha b) \ , \tag{B-56}$$

$$a_{7,3} = \frac{\mathrm{i}p}{b} \mathrm{J}_p(\beta b) \ , \tag{B-57}$$

$$a_{7,4} = \frac{\mathrm{i}p}{b} \mathrm{Y}_p(\beta b) \ , \tag{B-58}$$

$$a_{7,5} = \mathrm{i}k \, \mathrm{J}_{p+1}(\beta b) \ , \tag{B-59}$$

$$a_{7,6} = \mathrm{i}k \, \mathrm{Y}_{p+1}(\beta b) \ , \tag{B-60}$$

$$a_{7,7} = -a_{7,1} \ , \tag{B-61}$$

$$a_{7,8} = -a_{7,2} \ , \tag{B-62}$$

$$a_{7,9} = -a_{7,3} \ , \tag{B-63}$$

$$a_{7,10} = -a_{7,4} \ , \tag{B-64}$$

$$a_{7,11} = -a_{7,5} \ , \tag{B-65}$$

$$a_{7,12} = -a_{7,6} \ , \tag{B-66}$$

$$a_{8,1} = \frac{\mathrm{i}p}{b} \mathrm{J}_p(\alpha b) \ , \tag{B-67}$$

$$a_{8,2} = \frac{\mathrm{i}p}{b} \mathrm{Y}_p(\alpha b) \ , \tag{B-68}$$

$$a_{8,3} = \beta \, \mathrm{J}_{p+1}(\beta b) - \frac{p}{b} \mathrm{J}_p(\beta b) \ , \tag{B-69}$$

$$a_{8,4} = \beta \, \mathrm{Y}_{p+1}(\beta b) - \frac{p}{b} \mathrm{Y}_p(\beta b) \ , \tag{B-70}$$

$$a_{8,5} = \mathrm{i}k \, \mathrm{J}_{p+1}(\beta b) \ , \tag{B-71}$$

$$a_{8,6} = \mathrm{i}k \, \mathrm{Y}_{p+1}(\beta b) \ , \tag{B-72}$$

$$a_{8,7} = -a_{8,1} \ , \tag{B-73}$$

$$a_{8,8} = -a_{8,2} \ , \tag{B-74}$$

$$a_{8,9} = -a_{8,3} \ , \tag{B-75}$$

$$a_{8,10} = -a_{8,4} \ , \tag{B-76}$$

$$a_{8,11} = -a_{8,5} \ , \tag{B-77}$$

$$a_{8,12} = -a_{8,6} \ , \tag{B-78}$$

$$a_{9,1} = \mathrm{i}k \, \mathrm{J}_p(\alpha b) \ , \tag{B-79}$$

$$a_{9,2} = \mathrm{i}k \, \mathrm{Y}_p(\alpha b) \ , \tag{B-80}$$

$$a_{9,5} = \frac{(1-\mathrm{i})p}{b} \mathrm{J}_{p+1}(\beta b) - \beta \, \mathrm{J}_p(\beta b) \ , \tag{B-81}$$

$$a_{9,6} = \frac{(1-\mathrm{i})p}{b} \mathrm{Y}_{p+1}(\beta b) - \beta \, \mathrm{Y}_p(\beta b) \ , \tag{B-82}$$

$$a_{9,7} = -a_{9,1} \ , \tag{B-83}$$

$$a_{9,8} = -a_{9,2} \ , \tag{B-84}$$

$$a_{9,11} = -a_{9,5} \ , \tag{B-85}$$

$$a_{9,12} = -a_{9,6} \ , \tag{B-86}$$

$$a_{10,7} = \frac{2\mu\alpha}{c} \mathrm{J}_{p+1}(\alpha c) + \left[\frac{2\mu p(p-1)}{c^2} - \alpha^2(\lambda + 2\mu) - \lambda k^2 \right] \mathrm{J}_p(\alpha c) \ , \tag{B-87}$$

$$a_{10,8} = \frac{2\mu\alpha}{c} \mathrm{Y}_{p+1}(\alpha c) + \left[\frac{2\mu p(p-1)}{c^2} - \alpha^2(\lambda + 2\mu) - \lambda k^2 \right] \mathrm{Y}_p(\alpha c) \ , \tag{B-88}$$

$$a_{10,9} = \frac{-2\mathrm{i}\mu\beta p}{c} \mathrm{J}_{p+1}(\beta c) + \frac{2\mathrm{i}\mu p(p-1)}{c^2} \mathrm{J}_p(\beta c) \ , \tag{B-89}$$

$$a_{10,10} = \frac{-2\mathrm{i}\mu\beta p}{c} \mathrm{Y}_{p+1}(\beta c) + \frac{2\mathrm{i}\mu p(p-1)}{c^2} \mathrm{Y}_p(\beta c) \ , \tag{B-90}$$

$$a_{10,11} = \frac{-2\mathrm{i}\mu k(p+1)}{c} \mathrm{J}_{p+1}(\beta c) + 2\mathrm{i}\mu\beta k \, \mathrm{J}_p(\beta c) \ , \tag{B-91}$$

$$a_{10,12} = \frac{-2\mathrm{i}\mu k(p+1)}{c} \mathrm{Y}_{p+1}(\beta c) + 2\mathrm{i}\mu\beta k \, \mathrm{Y}_p(\beta c) \ , \tag{B-92}$$

$$a_{11,7} = \frac{-2\mathrm{i}\mu\alpha p}{c} \mathrm{J}_{p+1}(\alpha c) + \frac{2\mathrm{i}\mu p(p-1)}{c^2} \mathrm{J}_p(\alpha c) \ , \tag{B-93}$$

$$a_{11,8} = \frac{-2\mathrm{i}\mu\alpha p}{c} \mathrm{Y}_{p+1}(\alpha c) + \frac{2\mathrm{i}\mu p(p-1)}{c^2} \mathrm{Y}_p(\alpha c) \ , \tag{B-94}$$

$$a_{11,9} = \frac{-2\mu\beta}{c} \mathrm{J}_{p+1}(\beta c) + \left[\frac{-2\mu p(p-1)}{c^2} + \mu\beta^2 \right] \mathrm{J}_p(\beta c) \ , \tag{B-95}$$

$$a_{11,10} = \frac{-2\mu\beta}{c} \mathrm{Y}_{p+1}(\beta c) + \left[\frac{-2\mu p(p-1)}{c^2} + \mu\beta^2 \right] \mathrm{Y}_p(\beta c) \ , \tag{B-96}$$

$$a_{11,11} = \left[\frac{-\mu k p(1+\mathrm{i}) - 2\mathrm{i}\mu k}{c} \right] \mathrm{J}_{p+1}(\beta c) + \mathrm{i}\mu\beta k \, \mathrm{J}_p(\beta c) \ , \tag{B-97}$$

$$a_{11,12} = \left[\frac{-\mu k p(1+\mathrm{i}) - 2\mathrm{i}\mu k}{c} \right] \mathrm{Y}_{p+1}(\beta c) + \mathrm{i}\mu\beta k \, \mathrm{Y}_p(\beta c) \ , \tag{B-98}$$

$$a_{12,7} = -2\mathrm{i}k\mu\alpha \, \mathrm{J}_{p+1}(\alpha c) + \frac{2\mathrm{i}\mu k p}{c} \mathrm{J}_p(\alpha c) \ , \tag{B-99}$$

$$a_{12,8} = -2\mathrm{i}k\mu\alpha \, \mathrm{Y}_{p+1}(\alpha c) + \frac{2\mathrm{i}\mu k p}{c} \mathrm{Y}_p(\alpha c) \ , \tag{B-100}$$

$$a_{12,9} = \frac{-\mu k p}{c} \mathrm{J}_p(\beta c) \ , \tag{B-101}$$

$$a_{12,10} = \frac{-\mu k p}{c} \mathrm{Y}_p(\beta c) \ , \tag{B-102}$$

$$a_{12,11} = \left[\frac{\mu(\mathrm{i}-1)p(p+2)}{c^2} + \mu(\beta^2 - k^2) \right] \mathrm{J}_{p+1}(\beta c) - \frac{\mathrm{i}\mu\beta p}{c} \mathrm{J}_p(\beta c) \ , \tag{B-103}$$

and

$$a_{12,12} = \left[\frac{\mu(\mathrm{i}-1)p(p+2)}{c^2} + \mu(\beta^2 - k^2) \right] \mathrm{Y}_{p+1}(\beta c) - \frac{\mathrm{i}\mu\beta p}{c} \mathrm{Y}_p(\beta c) \ . \tag{B-104}$$

The nonzero entries of $[\mathbf{F}(n, p)]$ are

$$f_{4,1} = \frac{\omega^2 M_s}{2\pi b} \exp[\mathrm{i}(n-p)\theta_0] \left[-\alpha \, \mathrm{J}_{n+1}(\alpha b) + \frac{n}{b} \mathrm{J}_n(\alpha b) \right], \tag{B-105}$$

$$f_{4,2} = \frac{\omega^2 M_s}{2\pi b} \exp[\mathrm{i}(n-p)\theta_0] \left[-\alpha \, \mathrm{Y}_{n+1}(\alpha b) + \frac{n}{b} \mathrm{Y}_n(\alpha b) \right], \tag{B-106}$$

$$f_{4,3} = \frac{\omega^2 M_s}{2\pi b} \exp[\mathrm{i}(n-p)\theta_0] \left[\frac{\mathrm{i}n}{b} \mathrm{J}_n(\beta b) \right], \tag{B-107}$$

$$f_{4,4} = \frac{\omega^2 M_s}{2\pi b} \exp[\mathrm{i}(n-p)\theta_0] \left[\frac{\mathrm{i}n}{b} \mathrm{Y}_n(\beta b) \right], \tag{B-108}$$

$$f_{4,5} = \frac{\omega^2 M_s}{2\pi b} \exp[\mathrm{i}(n-p)\theta_0] \left[\mathrm{i}k \, \mathrm{J}_{n+1}(\beta b) \right], \tag{B-109}$$

$$f_{4,6} = \frac{\omega^2 M_s}{2\pi b} \exp[\mathrm{i}(n-p)\theta_0] \left[\mathrm{i}k \, \mathrm{Y}_{n+1}(\beta b) \right], \tag{B-110}$$

$$f_{5,1} = \frac{\omega^2 M_s}{2\pi b} \exp[\mathrm{i}(n-p)\theta_0] \left[\frac{\mathrm{i}n}{b} \mathrm{J}_n(\alpha b) \right], \tag{B-111}$$

$$f_{5,2} = \frac{\omega^2 M_s}{2\pi b} \exp[\mathrm{i}(n-p)\theta_0] \left[\frac{\mathrm{i}n}{b} \mathrm{Y}_n(\alpha b) \right], \tag{B-112}$$

$$f_{5,3} = \frac{\omega^2 M_s}{2\pi b} \exp[\mathrm{i}(n-p)\theta_0] \left[\beta \, \mathrm{J}_{n+1}(\beta b) - \frac{n}{b} \mathrm{J}_n(\beta b) \right], \tag{B-113}$$

$$f_{5,4} = \frac{\omega^2 M_s}{2\pi b} \exp[\mathrm{i}(n-p)\theta_0] \left[\beta \, \mathrm{Y}_{n+1}(\beta b) - \frac{n}{b} \mathrm{Y}_n(\beta b) \right], \tag{B-114}$$

$$f_{5,5} = \frac{\omega^2 M_s}{2\pi b} \exp[\mathrm{i}(n-p)\theta_0] \left[\mathrm{i}k\, \mathrm{J}_{n+1}(\beta b)\right] , \tag{B-115}$$

$$f_{5,6} = \frac{\omega^2 M_s}{2\pi b} \exp[\mathrm{i}(n-p)\theta_0] \left[\mathrm{i}k\, \mathrm{Y}_{n+1}(\beta b)\right] . \tag{B-116}$$

$$f_{6,1} = \left[\frac{A_s \rho_s \omega^2 - A_s E_s k^2}{2\pi b}\right] \exp[\mathrm{i}(n-p)\theta_0] \left[\mathrm{i}k\, \mathrm{J}_n(\alpha b)\right] , \tag{B-117}$$

$$f_{6,2} = \left[\frac{A_s \rho_s \omega^2 - A_s E_s k^2}{2\pi b}\right] \exp[\mathrm{i}(n-p)\theta_0] \left[\mathrm{i}k\, \mathrm{Y}_n(\alpha b)\right] , \tag{B-118}$$

$$f_{6,5} = \left[\frac{A_s \rho_s \omega^2 - A_s E_s k^2}{2\pi b}\right] \exp[\mathrm{i}(n-p)\theta_0] \left[\frac{(1-\mathrm{i})n}{b} \mathrm{J}_{n+1}(\beta b) - \beta\, \mathrm{J}_n(\beta b)\right] , \tag{B-119}$$

and

$$f_{6,6} = \left[\frac{A_s \rho_s \omega^2 - A_s E_s k^2}{2\pi b}\right] \exp[\mathrm{i}(n-p)\theta_0] \left[\frac{(1-\mathrm{i})n}{b} \mathrm{Y}_{n+1}(\beta b) - \beta\, \mathrm{Y}_n(\beta b)\right] , \tag{B-120}$$

The nonzero entry of **p** is

$$p_{10,1} = P_0 . \tag{B-121}$$

APPENDIX C
LIST OF SYMBOLS

$\hat{\mathbf{A}}$	Dynamic shell matrix
$\mathbf{A}(p)$	Dynamic shell sub-matrix
A_m	Wave propagation coefficient
A_s	Cross sectional area of stiffener
a	Inner radius of cylinder
α	Modified wavenumber associated with the dilatational wave of the cylinder
B_m	Wave propagation coefficient
b	Radial location of stiffener
β	Modified wavenumber associated with the shear wave of the cylinder
C_m	Wave propagation coefficient
c	Outer radius of cylinder
c_d	Dilatational wave speed of cylinder
c_S	Shear wave speed of cylinder
D_m	Wave propagation coefficient
E_m	Wave propagation coefficient
E_s	Young's modulus of the stiffener
$\hat{\mathbf{F}}$	Stiffener force matrix
$\mathbf{F}(n,p)$	Stiffener force sub-matrix
F_m	Wave propagation coefficient
$f_r(b,\theta,z)$	Radial stress of the stiffener
$f_\theta(b,\theta,z)$	Circumferential stress of the stiffener
$f_z(b,\theta,z)$	Longitudinal stress of the stiffener
G_m	Wave propagation coefficient
H_m	Wave propagation coefficient
K_m	Wave propagation coefficient
k	Longitudinal wavenumber
L_m	Wave propagation coefficient
λ	First Lamé constant of cylinder
M_m	Wave propagation coefficient
M_s	Mass per unit length of the stiffener
m	Cylindrical mode number
μ	Second Lamé constant of cylinder
N_m	Wave propagation coefficient
$\mathbf{p}$	Load sub-vector
$\hat{\mathbf{p}}$	Load vector
P_0	Magnitude of applied pressure
p	Equation index

$p(\theta,z)$	Applied pressure at the exterior of the cylinder
r	Radial location on the cylinder
ρ	Cylinder density
ρ_s	Stiffener density
t	Time
θ	Angular location on the cylinder
θ_0	Angular position of stiffener
$\tau_{rr}(a,\theta,z)$	Normal stress in radial direction
$\tau_{r\theta}(a,\theta,z)$	Shear stress in radial-circumferential direction
$\tau_{rz}(a,\theta,z)$	Shear stress in radial-longitudinal direction
$u_j(r,\theta,z,t)$	Radial displacement of the jth layer
$v_j(r,\theta,z,t)$	Circumferential displacement of the jth layer
$w_j(r,\theta,z,t)$	Longitudinal displacement of the jth layer
ω	Frequency
$\hat{\mathbf{x}}$	Coefficient vector
$\mathbf{x}_p$	Coefficient sub-vector
z	Longitudinal location on the cylinder

INITIAL DISTRIBUTION LIST

Addressee	No. of Copies
Office of Naval Research (Code 321, M. Traweek)	1
Office of Naval Research (Code 333, J. Muench)	1
Georgia Institute of Technology (D. Trivett)	1
Weidlinger Associates (J. Cipolla)	1
Defense Technical Information Center	2
Center for Naval Analyses	1